Band-Dependent Quasiparticle Dynamics in the Hole-Doped Ba-122 Iron Pnictides

Darius H. Torchinsky[a], James W. McIver[a], David Hsieh[a], G. F. Chen[b], J. L. Luo[b], N. L. Wang[b], Nuh Gedik[*,a]

[a]*Department of Physics, Massachusetts Institute of Technology, Cambridge, MA 02139 USA*
[b]*Institute of Physics, Chinese Academy of Science, Beijing, 100080, P. R. China*

Abstract

We report on band-dependent quasiparticle dynamics in the hole-doped Ba-122 pnictides measured by ultrafast pump-probe spectroscopy. In the superconducting state of the optimal and over hole-doped samples, we observe two distinct relaxation processes: a fast component whose decay rate increases linearly with excitation density and a slow component whose relaxation is independent of excitation strength. We argue that these two components reflect the recombination of quasiparticles in the two hole bands through intraband and interband processes. We also find that the thermal recombination rate of quasiparticles increases quadratically with temperature in all samples. The temperature and excitation density dependence of the decays indicates fully gapped hole bands and nodal or very anisotropic electron bands.

Key words:
Electronic structure of pnictides, Optical spectroscopies
PACS: 74.25.Gz, 78.47.+p

1. Introduction

Since their discovery in early 2008 [1], the iron-pnictide superconductors have become one of the most intensely researched topics within the condensed matter community. Nevertheless, a number of fundamental issues remain controversial, one of the most prominent of which is the structure of the superconducting gap. While Angle Resolved Photoemission Spectroscopy (ARPES) measurements have revealed nearly isotropic gap structure [2, 3], NMR [4] and penetration depth measurements [5] have both provided evidence of nodes via a power law dependence in temperature of their primary observable quantities.

The presence of five bands crossing the Fermi surface [2, 3, 6, 7] (three hole bands at zone center Γ and two at zone corner M) has also complicated theoretical efforts to describe pnictide superconductivity. The proposals for gap symmetry are myriad, including the extended s-wave sign-changing $s_{\pm}$ gap proposed by Mazin and coworkers [7], an order parameter that may either be $s_{\pm}$ with nodes on the electron pockets or $d_{x^2-y^2}$ with nodes on the holes pockets depending on the doping, as put forth by Graser et al. [8], or a d_{xy} state with nodes on the electron pockets and the hole pockets of the Fermi surface due to Yanagi et al. [9]. At the heart of the discrepancies between these proposals is the nature of the intra and interband interactions of the electrons.

These interactions may be probed by the use of ultrafast time-resolved optical pump-probe spectroscopy. In these experiments, a single pulse from a short-pulse laser system is split two separate beams, pump and the probe. The pump pulse injects nonequilibrium quasiparticle (QP) excitations into the sample while the probe beam interrogates the time-resolved dynamics of the QP population n. This is accomplished by monitoring the evolution of the change in reflectivity $\Delta R/R$, which is assumed proportional to n. Prior pump-probe measurements on the cuprate superconductors have provided information on gap symmetry and recombination dynamics [10, 11, 12], while studies in the pnictides have shown evidence of a pseudogap state [13] and competing electronic order [14].

In this work, we apply pump-probe methods to the optimally and overdoped Ba-122 pnictides in the hole-doped side of the phase diagram in order to study nonequilibrium quasiparticle recombination in a band-dependent manner. We find that our reflectivity traces below T_c are comprised of a fast component whose decay rate depends linearly upon incident pump fluence Φ (indicating bimolecular recombination) and a slow, "bottlenecked" component which is independent of the excitation strength for all samples. ARPES data [2] and LDA calculations [15] allow assignment of the fast component to the two innermost hole pockets and the slow component to the outer hole pocket while the electron pockets are optically dark at our probe wavelength. Further analysis reveals that the thermal population of QPs n_{th} goes as T^2, while the scaling of the number of QPs with excitation fluence Φ is linear, indicating fully gapped bands in the optically interrogated portion of the Fermi surface. Taken as a whole, those observations point towards models which predict fully gapped hole bands and nodal or very anisotropic gaps in the electron pockets.

*Corresponding author.
Email address: gedik@mit.edu (Nuh Gedik)

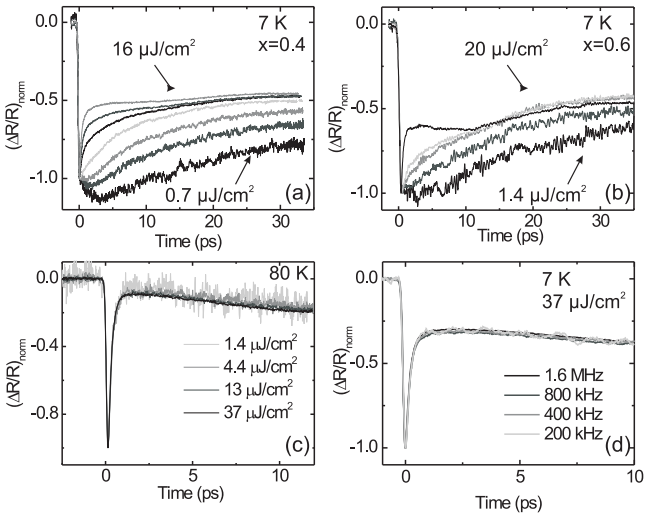

Figure 1: Normalized reflectivity transients $(\Delta R/R)_{norm}$ at different absorbed pump fluences (Φ) at 7 K for $x = 0.4$. At 7 K, the decay rate of the transients increases systematically with increasing fluence (from bottom to top: Φ = 0.7 μJ/cm^2, 2.2, 4.4, 7.0, 8.9, 12.8 to 16.1 μJ/cm^2). (b) A similar trend is observed for an overdoped ($x = 0.6$) compound (from bottom to top: Φ = 1.4 μJ/cm^2, 2.2, 4.4, 7.0, 13 to 20 μJ/cm^2). (c) At 80 K, the dynamics do not depend on Φ. (d) $(\Delta R/R)_{norm}$ measured at four different repetition rates are identical, verifying the absence of cumulative heating ($x = 0.4$, Φ = 37 μJ/cm^2 and T=7 K).

2. Results and Discussion

For this study, we used a Ti:sapphire oscillator producing pulses with center wavelength 795 nm ($h\nu$ = 1.56 eV) and duration 60 fs at FWHM. The 80 MHz repetition rate was reduced to 1.6 MHz with a pulse picker to eliminate steady state heating of the sample. Both beams were focussed on the sample to 60 μm FWHM spots and the probe beam reflected back to an amplified photodiode for detection. Use of a double-modulation scheme [10] provided sensitivity of the fractional change in reflectivity of $\Delta R/R \sim 10^{-7}$. The pump fluence Φ was varied with neutral density filters in order to tune the QP excitation density. High-quality single crystals of $Ba_{1-x}K_xFe_2As_2$ (x = 0.4, 0.5, 0.6) were grown by the self-flux method [16]. SQUID magnetometry measurements yielded a very sharp transition ($\Delta T \approx 1$ K) at T_c = 37 K for all samples, indicating a high degree of sample purity.

Figures 1a and 1b show reflectivity transients at 7 K in optimally doped and overdoped $Ba_{1-x}K_xFe_2As_2$ samples, respectively, for a variety of pump fluences. The observed behavior in the traces is qualitatively the same: there is an initial decrease in $(\Delta R/R)_{norm}$ coincident with the arrival of the pump pulse at time $t = 0$, followed by a recovery of the signal, whose rate decreases with Φ. After this initial intensity dependent relaxation, $\Delta R/R$ tends towards a constant offset indicating the existence of a much longer lived set of dynamics. Above 60 K, we observe data collapse of the normalized traces indicating that the recovery dynamics are independent of the pump fluence, shown here at 80 K in Figure 1c. From the data in Figures 1a-c, we conclude that the decay rate increases both with increasing temperature and excitation density. In order to rule out steady state

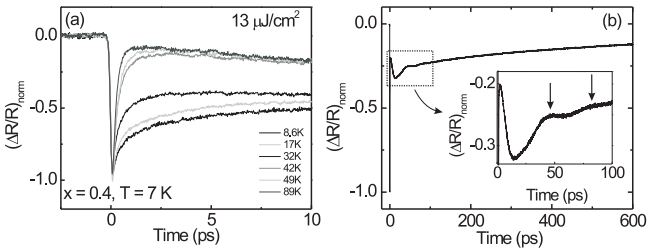

Figure 2: (a) Temperature dependence of the normalized reflectivity transients near T_c obtained at Φ=13 μJ/cm^2. Above T_c there is an upturn of the signal evident at short time delays which disappears below T_c. We also note a sharp decrease in the offset across the transition (i.e. 32 K to 42 K). (b) Dynamics of the decay measured for a longer time window at T=8 K and Φ=37 μJ/cm^2. Highly damped oscillations are observed with a period of ~40 ps due to Stimulated Brillouin Scattering (inset).

heating as the source of this intensity dependence, we used a pulse picker to vary the repetition rate. Figure 1d shows 7 K transients taken with $\Phi = 37\mu J/cm^2$ at repetition rates ranging from 200 kHz to 1.6 MHz, where we observe no discernible change in the recovery dynamics.

In Fig. 2a, we plot the temperature dependence of transients at Φ=13 μJ/cm^2. As the system is warmed above T_c, the decay rate continues to increase until ~60 K, above which the traces superpose. At T_c, we observe a sudden disappearance of the offset, indicating its origin in superconductivity. At temperatures above T_c, we observe the appearance of a component that continues to rise within the 10 ps measurement window. The same upturn behavior is also observed below T_c at the highest fluences (e.g., Figure 1d). In order to examine this feature further, the measurement window was extended to times long enough to capture its recovery, as shown in Fig. 2b. We observe that the upturn in the signal is the beginning of strongly damped oscillations of period ~40 ps, attributable to stimulated Brillouin scattering [17], while the offset is seen to decay exponentially on the time scale of ~700 ps.

Both the slow and fast components of the recovery dynamics described above may be understood withing the framework of the Rothwarf-Taylor equations [18]

$$\dot{n} = I_{qp} + 2\gamma_{pc}N - Bn^2 \quad (1)$$

$$\dot{N} = I_{ph} + Bn^2/2 - \gamma_{pc}N - (N - N_{eq})\gamma_{esc}. \quad (2)$$

Here, n is the QP number density, N is the boson number density, I_{qp} and I_{ph} are the external QP and boson generation rates, respectively, γ_{pc} is the pair creation rate via annihilation of gap energy bosons, N_{eq} is the equilibrium boson number density, γ_{esc} is the boson escape rate, and B is the bimolecular recombination constant. Depending upon the relative magnitudes of the three rates Bn, γ_{pc} and γ_{esc}, the solutions of these equations display different characteristics. In the limit where $\gamma_{esc} \ll \gamma_{pc}$, Bn (i.e. the phonon bottleneck), QPs and bosons come to a quasiequilibrium and the combined population decays with a slow rate proportional to γ_{esc} and the recombination is said to be "bottlenecked." This corresponds to the case observed for the slow component of the signal, depicted in Figure 2a.

In the limit that $Bn/\gamma_{pc} \gg 1$, however, the pairing boson cannot regenerate the QP pair and equations (1) and (2) decouple.

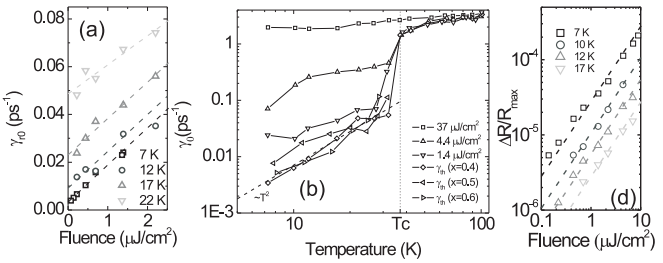

Figure 3: (a) The initial decay rate (γ_{r0}) as a function of pump fluence at various temperatures in the optimally doped sample ($x = 0.4$). Dashed lines show linear fits to data, as described in the text. The thermal decay rate (γ_{th}) at each temperature was obtained by extrapolating the fits to zero fluence. (b) The initial relaxation rate γ_0 plotted as a function of temperature for three representative pump fluences along with the thermal rate γ_{th} for all samples studied here ($x = 0.4$, $x = 0.5$, $x = 0.6$). Below T_c, γ_0 strongly depends on the excitation density. There is a sharp transition at 37 K, although a discernable intensity dependence persists above T_c. The dashed line shows T^2 dependence as a guide. (c) $|(\Delta R/R)_{max}|$ plotted as a function of Φ for four temperatures, each offset for clarity. Dashed lines show a slope of one.

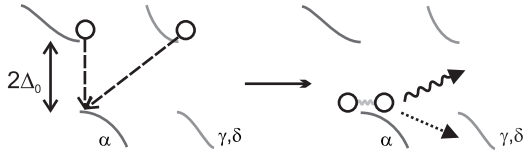

Figure 4: Schematic representation of interband QP recombination. When QPs in α and γ,δ recombine, a Cooper pair is produced and an optical phonon and antiferromagnetic spin fluctuation are emitted.

The QP density relaxes through simple bimolecular recombination ($dn/dt = -Bn^2$) as is observed for the fast component of the signal in Figures 1a and 1b. In this decoupled regime, the RT equations permit determination of the thermal decay rate of QPs (γ_{th}) and B. By writing $n = n_{ph} + n_{th}$, equation (1) becomes $dn/dt = -Bn_{ph}^2 - 2Bn_{ph}n_{th}$ [10], where n_{ph} (n_{th}) is the photoinduced (thermal) QP population. We consider the initial recombination rate $\gamma_0 = -(1/n_{ph})(dn_{ph}/dt)|_{t\to 0} = Bn_{ph} + 2Bn_{th} = \gamma_{ph} + 2\gamma_{th}$, where $\gamma_{ph,th} = Bn_{ph,th}$. Experimentally, γ_0 is deduced from the initial slope of the transients following the peak. Figure 3a plots γ_0 versus Φ in the low excitation regime for four representative temperatures in the optimally doped sample. For each temperature, we obtain γ_{th} by extrapolating the linear fits to zero excitation density (i.e. $n_{ph} \propto \Phi \to 0$). The slope of the fits is proportional to B which does not strongly depend on the temperature while the intercept γ_{th} increases with T due to the greater thermal QP population.

Figure 3b presents the temperature dependence of γ_0 at various fluences both in the high and low fluence regimes along with the extrapolated thermal rate γ_{th} in all samples studied here. We observe strong dependence of γ_0 on the excitation density below T_c which diminishes markedly at T_c. There is remnant intensity dependence above 37 K that is seen to persist to ~ 60 K. Significantly, we note that the thermal decay rate depends quadratically on temperature ($\gamma_{th} = Bn_{th} \propto T^2$) below T_c. This is suggestive of a node in the gap around which $n_{th} \propto T^2$ as opposed to the exponential dependence $T \propto \exp -\Delta/k_bT$ expected from an isotropic gap. Figure 3b also reveals that the thermal decay rate $Bn_{th} \propto T^2$ below T_c for both of the overdoped samples studied here. The consistency of the observed power law with doping suggests that the shape of the Fermi surface in the neighborhood of such a possible node does not change appreciably with the addition of holes.

An additional characterization of the Fermi surface topology is afforded by the dependence of the initial magnitude of the reflectivity transients $\Delta R(0)/R$ on the amount of energy deposited in the system. In the case that the excitations are fully gapped, the amount of energy required to generate the quasiparticles is simply proportional to the absorbed energy. In this case, we should observe $\Delta R(0)/R \propto \Phi$. When there is a line node somewhere within the gap, the fact that the density of states depends linearly on energy near the node results in a $\Delta R(0)/R \propto \Phi^{2/3}$ dependence of the signal. Fig. 3c shows the amplitude of $\Delta R/R$ as a function of Φ at low fluence for four temperatures, where a clear linear dependence is observed at all temperatures, indicating that the photoinduced QPs all originate from fully gapped excitations.

The simultaneous observation of nodal (i.e. $n_{th} \propto T^2$) and fully gapped (i.e. $n \propto \Phi$) characteristics in our data may be traced to the multiband nature of pnictides mentioned above. We attribute the entirety of the observed signal to the two hole pockets at Γ, (i.e., the inner hole bands α and outer hole band β, using the nomenclature of [19]). Neither of the electron bands at M (γ and δ) contribute significantly to the signal as LDA calculations [15] reveal a dearth of accessible states 1.5 eV above and (properly renormalized [3]) below the Fermi level at this point in the Brillouin zone, rendering QP recombination there optically dark at our probe wavelength. Furthermore, an estimate of the Sommerfeld parameter shows that the density of states at β and at the combination of the two bands at α are each 7 times larger than at γ and δ [19], with the implication that the number of photoinduced QPs in the hole pockets should overwhelm that of the electron pockets.

The band structure and possible QP relaxation channels allow assignment of the fast dynamics to the α band and the slow component to β. The observation of a dispersion kink in ARPES measurements at 25 meV that appears in α and γ,δ but not β [3, 20] indicates a strong coupling between α and γ,δ by an excitation at 13 meV, interpreted to be a resonant magnetic excitation [21], and which arises due to their near-perfect Fermi surface nesting. This excitation makes it possible for the QPs in α to pair up with their counterparts in γ,δ through an interband process by emitting a combination of an optical phonon and a magnetic excitation (Figure 4). The inverse process, however, is necessarily very slow since three-body scattering of an antiferromagnetic spin fluctuation, an optical phonon and a Cooper pair is required to generate QPs. The short lifetime of the magnetic mode, as indicated by its relatively broad energy linewidth [21], further inhibits the reverse process, leading to a small value of γ_{pc} which prevents formation of a bottleneck in the interband channel. In the case of intraband recombination in α, which occurs by emission of an A_{1g} optical phonon ($E = 2\Delta_0 = 24$ meV), the phonon's short lifetime (3 ps)[22] precludes it, too, from generating a bottleneck. We therefore

ascribe the intensity dependent decay to the non-bottlenecked bare quasiparticle recombination in α and the slow dynamics to a boson bottleneck in β.

These assignments allow for a proper interpretation of the simultaneous observation of T^2 behavior for n_{th} and the linear dependence of $\Delta R/R$ on Φ. The thermal QPs participating in the observed recombination at low fluences are not necessarily the same as the photoinduced ones; rather, they may also originate from either γ or δ. A line node in either γ or δ will lead to a preponderance of thermally excited QPs from the electron bands as compared with the fully gapped hole bands. These QPs will then dominate the recombination process which, in tandem with the interband recombination process described above, can account for the observed behavior in its entirety. While another possibility for the quadratic temperature dependence of n_{th} is the proposed $s_{\pm}$ gap symmetry with interband impurity scattering, this scenario can only be realized within a very specific range of impurity parameters [6]. Therefore, while we cannot definitively differentiate between the two scenarios at present, our results are highly suggestive of nodes in the electron pockets.

3. Conclusion

In summary, we have presented time resolved measurements of band dependent QP dynamics in optimally doped and overdoped samples of $Ba_{1-x}K_xFe_2As_2$. Below T_c, we find that the rate of QP recombination increases linearly with excitation density indicating pairwise recombination within the inner hole band. The number of photoinduced QPs increases linearly with excitation density indicating the fully gapped nature of the hole bands. Meanwhile, the dynamics within the outer hole band exhibit bottlenecked recombination. We have observed that the thermal recombination rate of QPs varies as T^2. We posit that this arises from a line node in the electron bands although we cannot definitively rule out the $s_{\pm}$ order parameter with interband impurity scattering at this time.

The authors thank Dr. Deepak Singh for assistance with SQUID magnetometry measurements and Prof. B. Andrei Bernevig for useful discussions. This work was supported primarily by DOE Grant No. DE-FG02-08ER46521 and in part by the MRSEC Program of the National Science Foundation under award number DMR - 0819762, NSFC, CAS and project 973 of the MOST of China.

References

[1] Y. Kamihara, T. Watanabe, M. Hirano, and H. Hosono, J. Am. Chem. Soc. **130**, 3296 (2008).
[2] H. Ding *et al.*, Europhys. Lett.**83**, 47001 (2008).
[3] L. Wray *et al.*, Phys. Rev. B **78**, 184508 (2008).
[4] H. Fukazawa *et al.*, J. Phys. Soc. Jpn. **78**, 033704 (2009).
[5] C. Martin *et al.*, Phys. Rev. B **80**, 020501 (2009).
[6] A. V. Chubukov, D. V. Efremov, and I. Eremin, Phys. Rev. B **78**,134512 (2008).
[7] I. I. Mazin, D. J. Singh, M. D. Johannes, and M. H. Du, Phys. Rev. Lett. **101**, 057003 (2008).
[8] S. Graser, T. A. Maier, P. J. Hirschfeld, and D. J. Scalapino, New Journal of Physics **11**, 025016 (2009).
[9] Y. Yanagi, Y. Yamakawa, and Y. Ono,J. Phys. Soc. of Jpn. **77**, 123701 (2008).
[10] N. Gedik, P. Blake, R. C. Spitzer, J. Orenstein, R. Liang, D. A. Bonn, and W. N. Hardy, Phys. Rev. B **70**, 014504 (2004).
[11] N. Gedik, M. Langner, J. Orenstein, S. Ono, Y. Abe, and Y. Ando, Phys. Rev. Lett. **95**, 117005 (2005).
[12] J. Demsar, R. D. Averitt, A. J. Taylor, V. V. Kabanov, W. N. Kang, H. J. Kim, E. M. Choi, and S. I. Lee, Phys. Rev. Lett. **91**, 267002 (2003).
[13] T. Mertelj, V. V. Kabanov, C. Gadermaier, N. D. Zhigadlo, S. Katrych, J. Karpinski, and D. Mihailovic, Phys. Rev. Lett. **102**, 117002 (2009).
[14] E. E. M. Chia *et al.*, Phys. Rev. Lett. **104**, 027003 (2010).
[15] F. Ma, Z.-Y. Lu, and T. Xiang, arXiv:0806.3526 (2008).
[16] G. F. Chen *et al.*, Phys. Rev. B **78**, 224512 (2008).
[17] C. Thomsen, H. T. Grahn, H. J. Maris, and J. Tauc, Phys. Rev. B **34**, 4129 (1986).
[18] A. Rothwarf and B. N. Taylor, Phys. Rev. Lett. **19**, 27 (1967).
[19] H. Ding *et al.*, arXiv:0812.0534 (2008).
[20] P. Richard *et al.*, Phys. Rev. Lett. **102**, 047003 (2009).
[21] A. D. Christianson *et al.*, Nature **456**, 930 (2008).
[22] B. Mansart, D. Boschetto, A. Savoia, F. Rullier-Albenque, A. Forget, D. Colson, A. Rousse, M. Marsi, Phys. Rev. B **80**, 172504 (2009).